

Neutrino Propagation In Color Superconducting Quark Matter

Gregory W. Carter¹ and Sanjay Reddy²

¹*Department of Physics and Astronomy, SUNY Stony Brook, NY 11794-3800.*

²*Institute For Nuclear Theory, University of Washington, Seattle, WA 98195.*

(October 28, 2018)

We calculate the neutrino mean free path in color superconducting quark matter, and employ it to study the cooling of matter via neutrino diffusion in the superconducting phase as compared to a free quark phase. The cooling process slows when quark matter undergoes a second order phase transition to a superconducting phase at the critical temperature T_c . Cooling subsequently accelerates as the temperature decreases below T_c . This will directly impact the early evolution of a newly born neutron star, should its core contain quark matter. Consequently, there may be observable changes in the early neutrino emission which would provide evidence for superconductivity in hot and dense matter.

I. INTRODUCTION

In this article we study heat diffusion via neutrinos in dense, color superconducting quark matter. Recent theoretical works [1–6] suggest that quarks form Cooper pairs in medium, a natural consequence of attractive interactions destabilizing the Fermi surface. This would likely affect the early evolution of neutron stars born through a Type II supernova explosion, where the central role of neutrino diffusion through a strongly-interacting medium has long been postulated on theoretical grounds [8].

Type II (core collapse) supernovae are triggered by the implosion of the inner core of a massive star ($M_{\text{star}} \sim 8 - 20 M_{\odot}$), when the core mass is on the order of the Chandrasekhar mass ($M_{\text{core}} \simeq 1.4 M_{\odot}$). During the implosion nearly all ($\sim 99\%$) of the enormous gravitational binding energy ($\sim 10^{53}$ ergs) gained is stored as internal energy of the newly born, proto-neutron star (PNS). The subsequent evolution of the proto-neutron star is driven by neutrino diffusion. Temporal and spectral characteristics of the neutrino emission depend on the rate at which neutrinos diffuse through the imploded PNS which, at this early stage, is composed of hot ($T \sim 20 - 30$ MeV) and dense ($n_B \sim 2 - 3 n_0$ where $n_0 = 0.16 \text{ fm}^{-3}$) strongly-interacting matter.

Neutrino emission during this phase is a directly observable feature of a galactic supernova explosion. The few neutrinos detected from SN 1987A indicate that neutrinos of mean energy $\langle E_{\nu} \rangle \sim 20$ MeV are emitted on a diffusion time scale of about 10 – 20 seconds. It is reasonable to expect that neutrino mean free path in the inner, denser regions of the star will strongly influence the temporal characteristics of a supernova neutrino signal. Supernova neutrinos can therefore reveal properties of matter at high baryon density, at temperatures substantially lower than those expected in relativistic heavy ion collisions.

Although the idea of quark pairing in dense matter is not a new one [1], it has recently seen renewed interest in the context of the phase diagram of QCD [2]. Model calculations, mostly based on four-quark effective interactions, predict the restoration of spontaneously broken chiral symmetry through the onset of color superconductivity at low temperatures [3]. For much higher densities color superconductivity is manifest through perturbative gluon exchange [6,7], which can be calculated systematically suggests that the phenomenon is robust. For densities and temperatures relevant to neutron stars, quark matter is therefore expected to be superconducting. Models generally predict an energy gap of $\Delta \sim 100$ MeV for a typical quark chemical potential of $\mu_q \sim 400$ MeV. As in BCS theory, the gap will weaken for $T > 0$ and at some $T = T_c$ there is a (second-order) transition to a “standard” quark-gluon plasma. Thus, when cooling from temperatures greater than critical, the formation of a such a gap in the fermionic excitation spectrum in quark matter at high density will influence various neutron star observables – if neutron stars contain quark matter in their cores at early time¹. Two examples recently investigated are the effects on magnetic fields [10] and on the thermal evolution of neutron stars at late time [11], when interior temperatures evolve from $T \sim 1$ MeV to $T \lesssim 1$ KeV. In this work we shall consider the cooling of quark matter at earlier times, when temperatures pass

¹ This remains unclear. In particular, the existence of a finite electron neutrino chemical potential at very early time has shown to inhibit the appearance of quark matter. See Ref. [9] for a review.

through the critical $T_c \sim \Delta$. Assuming a simplified scenario, we investigate the thermal evolution of the inner core of a proto-neutron star as it cools via neutrino diffusion during its first few seconds.

Our main finding is that the neutrino mean free path in the superconducting phase has a strong dependence on temperature. An energy gap tends to increase the neutrino mean free paths exponentially when $T \ll \Delta$. However in the intermediate regime, when $T \sim \Delta$, the temperature dependence is not exponential. From this we predict a uniquely uneven cooling process for simplified PNS matter, marked by a slowdown of the cooling rate when the system undergoes a second-order phase transition. This is a consequence of the specific heat being peaked at T_c , a standard characteristic of a phase transition, rather than a large change in the neutrino mean free path. Since the energy gap vanishes at this point, the mean free path is *not* significantly modified in the neighborhood of T_c .

In Section II the neutrino mean free path, always denoted λ in this work, is computed in a background of superconducting quarks. Taking a general, BCS-type model for the energy gap, we relate λ to in-medium quark polarizations via the differential and total neutrino-quark cross sections. Explicit formulae are derived for the imaginary parts of the vector and axial-vector polarizations of a relativistic Fermi system with an energy gap. After assuming BCS-type mean field behavior of the gap and the specific heat, in Section III we compute a characteristic time for heat diffusion via neutrino emission from a simple model of superconducting quark matter. We then consider some astrophysical consequences and outline the model's applicability to proto-neutron stars. Section IV contains our conclusions.

II. NEUTRINO-QUARK SCATTERING IN A COLOR SUPERCONDUCTOR

The primary process by which heat escapes a proto-neutron star is neutrino diffusion, and so a significant consequence of color superconductivity in this context will be modified neutrino propagation. While noting that the neutrino production rate will also differ from that of normal matter, in the diffusive regime one can see that the dominant critical behavior will be a change in the *inelastic* quark-neutrino cross section, since here neutrino production rates decouple from the transport equation and depend only on the neutrino mean free path. In this section we calculate the differential and total cross sections and then compute the neutrino mean free path in two-flavor quark matter. The magnitude of the superconducting gap, Δ , is taken as arbitrary within a range of values found in recent literature. Closely following BCS theory, we assume the gap to be a constant, and calculate the response functions and neutrino cross sections in the weak coupling approximation.

The neutral current coupling between neutrinos and quarks, a four-fermion effective interaction for energies $E_\nu \ll M_Z$, is written as

$$\mathcal{L}_W = \frac{G_F}{\sqrt{2}} \bar{\nu} \gamma_\mu (1 - \gamma_5) \nu \bar{q} \gamma^\mu (C_V - C_A \gamma_5) q, \quad (1)$$

where $G_F = 1.166 \times 10^{-5} \text{ GeV}^{-2}$ is the Fermi weak coupling constant and C_V and C_A are the flavor-specific vector and axial vector coupling constants, respectively. The differential neutrino scattering cross section per unit volume in an infinite and homogeneous system of fermions as calculated in linear response theory is [12,13]

$$\frac{1}{V} \frac{d^3\sigma}{d^2\Omega_3 dE_3} = -\frac{G_F^2}{32\pi^2} \frac{E_3}{E_1} \frac{[1 - f_\nu(E_3)]}{[1 - \exp(-q_0/T)]} \text{Im} (L^{\alpha\beta} \Pi_{\alpha\beta}), \quad (2)$$

where E_1 (E_3) is the incoming (outgoing) neutrino energy. The factor $[1 - \exp(-q_0/T)]^{-1}$ maintains detailed balance and the final state blocking of the outgoing neutrino is enforced by the Pauli blocking factor, $[1 - f_\nu(E_3)]$. The neutrino tensor $L_{\alpha\beta}$ is given by

$$L^{\alpha\beta} = 8[2k^\alpha k^\beta + (k \cdot q)g^{\alpha\beta} - (k^\alpha q^\beta + q^\alpha k^\beta) \mp i\epsilon^{\alpha\beta\mu\nu} k_\mu q_\nu], \quad (3)$$

where the incoming four-momentum is k^α and the momentum transferred to the medium is q^α . The minus (plus) sign on the final term applies to neutrino (anti-neutrino) scattering.

The medium is characterized by the quark polarization tensor $\Pi_{\alpha\beta}$. In the case of free quarks, each flavor contributes a term of the form

$$\Pi_{\alpha\beta}(q) = -i \text{Tr}_c \int \frac{d^4p}{(2\pi)^4} \text{Tr} [S_0(p) \Gamma_\alpha S_0(p+q) \Gamma_\beta], \quad (4)$$

where $S_0(p)$ is the free quark propagator at finite chemical potential and temperature. The outer trace is over color and simplifies to a $N_c = 3$ degeneracy. The inner trace is over spin, and the Γ_α are the neutrino-quark vertex functions which determine the spin channel. Specifically, the vector polarization is computed by choosing $(\Gamma_\alpha, \Gamma_\beta) = (\gamma_\alpha, \gamma_\beta)$.

The axial and mixed vector-axial polarizations are similarly obtained from $(\Gamma_\alpha, \Gamma_\beta) = (\gamma_\alpha \gamma_5, \gamma_\beta \gamma_5)$ and $(\Gamma_\alpha, \Gamma_\beta) = (\gamma_\alpha, \gamma_\beta \gamma_5)$, respectively.

The free quark propagators in Eq. (4) are naturally modified in a superconducting medium. As first pointed out by Bardeen, Cooper, and Schrieffer several decades ago, the quasi-particle dispersion relation is modified due to the presence of a gap in the excitation spectrum. In calculating these effects, we will consider the simplified case of QCD with two quark flavors which obey $SU(2)_L \times SU(2)_R$ flavor symmetry, given that the light u and d quarks dominate low-energy phenomena. Furthermore we will assume that, through some unspecified effective interactions, quarks pair in a manner analogous to the BCS mechanism [14]. The relevant consequences of this are the restoration of chiral symmetry (hence all quarks are approximately massless) and the existence of an energy gap at zero temperature, Δ_0 , with approximate temperature dependence,

$$\Delta(T) = \Delta_0 \sqrt{1 - \left(\frac{T}{T_c}\right)^2}. \quad (5)$$

The critical temperature $T_c \simeq 0.57\Delta_0$ is likewise taken from BCS theory; this relation has been shown to hold for perturbative QCD [15] and is thus a reasonable assumption for non-perturbative physics.

Breaking the $SU_c(3)$ color group leads to complications not found in electrodynamics. In QCD the superconducting gap is equivalent to a diquark condensate, which can at most involve two of the three fundamental quark colors. The condensate must therefore be colored. Since the scalar diquark (in the $\mathbf{3}$ color representation) appears to always be the most attractive channel, we consider the anomalous (or Gorkov) propagator [5]

$$\begin{aligned} F(p)_{abfg} &= \langle q_{fa}^T(p) C \gamma_5 q_{gb}(-p) \rangle \\ &= -i\epsilon_{ab3}\epsilon_{fg}\Delta \left(\frac{\Lambda^+(p)}{p_o^2 - \xi_p^2} + \frac{\Lambda^-(p)}{p_o^2 - \bar{\xi}_p^2} \right) \gamma_5 C. \end{aligned} \quad (6)$$

Here, a, b are color indices, f, g are flavor indices, ϵ_{abc} is the usual anti-symmetric tensor and we have conventionally chosen 3 to be the condensate color. This propagator is also antisymmetric in flavor and spin, with $C = -i\gamma_0\gamma_2$ being the charge conjugation operator.

The color bias of the condensate forces a splitting of the normal quark propagator into colors transverse and parallel to the diquark. Quarks of color 3, parallel to the condensate in color space, will be unaffected and propagate freely, with

$$S_0(p)_{af}^{bg} = i\delta_a^b \delta_f^g \left(\frac{\Lambda^+(p)}{p_o^2 - E_p^2} + \frac{\Lambda^-(p)}{p_o^2 - \bar{E}_p^2} \right) (p_\mu \gamma^\mu - \mu \gamma_0). \quad (7)$$

This is written in terms of the particle and anti-particle projection operators $\Lambda^+(p)$ and $\Lambda^-(p)$ respectively, where $\Lambda^\pm(p) = (1 \pm \gamma_0 \vec{\gamma} \cdot \hat{p})/2$. The excitation energies are simply $E_p = |\vec{p}| - \mu$ for quarks and $\bar{E}_p = |\vec{p}| + \mu$ for anti-quarks.

On the other hand, transverse quark colors 1 and 2 participate in the diquark and thus their quasi-particle propagators are given as

$$S(p)_{af}^{bg} = i\delta_a^b \delta_f^g \left(\frac{\Lambda^+(p)}{p_o^2 - \xi_p^2} + \frac{\Lambda^-(p)}{p_o^2 - \bar{\xi}_p^2} \right) (p_\mu \gamma^\mu - \mu \gamma_0). \quad (8)$$

The quasi-particle energy is $\xi_p = \sqrt{(|\vec{p}| - \mu)^2 + \Delta^2}$, and for the anti-particle $\bar{\xi}_p = \sqrt{(|\vec{p}| + \mu)^2 + \Delta^2}$.

The appearance of an anomalous propagator in the superconducting phase indicates that the polarization tensor gets contributions from both the normal quasi-particle propagators (8) and anomalous propagator (6). Thus, to order G_F^2 , Eq. (4) is replaced with the two contributions corresponding to the diagrams shown in Fig. 1, and written

$$\Pi_{\alpha\beta}(q) = -i \int \frac{d^4 p}{(2\pi)^4} \left\{ \text{Tr} [S_0(p)\Gamma_\alpha S_0(p+q)\Gamma_\beta] + 2\text{Tr} [S(p)\Gamma_\alpha S(p+q)\Gamma_\beta] + 2\text{Tr} [F(p)\Gamma_\alpha \bar{F}(p+q)\Gamma_\beta] \right\}. \quad (9)$$

The remaining trace is over spin, as the color trace has been performed. Fig. 1(a) corresponds to the first two terms, which have been decomposed into one term with ungapped propagators (7) and the other with gapped quasi-particle propagators (8). Fig. 1(b) represents the third, anomalous term.

For neutrino scattering we must consider vector, axial, and mixed vector-axial channels, all summed over flavors. The full polarization, to be used in evaluating Eq. (2), may be written

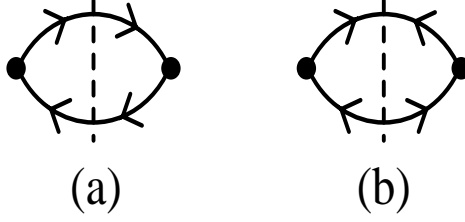


FIG. 1. Standard loop (a) and anomalous loop (b) diagrams contributing to the quark polarization operator.

$$\Pi_{\alpha\beta} = \sum_f \left[(C_V^f)^2 \Pi_{\alpha\beta}^V + (C_A^f)^2 \Pi_{\alpha\beta}^A - 2C_V^f C_A^f \Pi_{\alpha\beta}^{VA} \right]. \quad (10)$$

The coupling constants for up quarks are $C_V^u = \frac{1}{2} - \frac{4}{3} \sin^2 \theta_W$ and $C_A^u = \frac{1}{2}$, and for down quarks, $C_V^d = -\frac{1}{2} + \frac{2}{3} \sin^2 \theta_W$ and $C_A^d = -\frac{1}{2}$, where $\sin^2 \theta_W \simeq 0.23$ is the Weinberg angle.

If we specify a frame in which the transfer momentum is $q_\mu = (q_0, q, 0, 0)$ we can separate longitudinal components as

$$\Pi_L^V = -\frac{q_\mu^2}{q^2} \Pi_{00}^V = -\frac{q_\mu^2}{q_0^2} \Pi_{11}^V = -\frac{q_\mu^2}{q_0 q} \Pi_{10}^V, \quad (11)$$

and the transverse,

$$\Pi_T^V = \Pi_{22}^V = \Pi_{33}^V. \quad (12)$$

Identical definitions apply to the axial polarizations Π_L^A and Π_T^A . The non-zero mixed correlation function is written

$$\Pi_{\alpha\beta}^{VA} = i\epsilon_{\alpha\beta\mu 0} q^\mu \Pi^{VA}. \quad (13)$$

Detailed calculations of these polarization functions are given in the Appendix.

As the gap increases, the superconducting quasi-particles naturally become the dominant excitations of the background, a property clearly visible in the neutrino response functions. The left panel of Fig. 2 shows the longitudinal response in the vector channel. The free quark case, shown as a solid line labeled $\Delta = 0$, is the standard result describing Pauli-blocking and kinematics of massless single particle excitations [16]. Here, energy-momentum conservation restricts the response to the spacelike region ($q_0 < q$). Superconductivity modifies this result, as the quasi-quark excitations become suppressed due to the pairing correlations at the Fermi surface. At the same time, the response is enhanced when $q_0 \geq 2\Delta$, signifying the excitation of Cooper pairs. In particular, the results with greater Δ clearly show the threshold for these excitations at energy transfer $q_0 = 2\Delta$. Results for $\Delta = 10, 30$ and 50 MeV show the gradual reallocation of response strength from small q_0 to the region $q_0 \geq 2\Delta$. Since scattering probes only the spacelike region, the Π_{00}^V contribution to the cross section is generically *suppressed* in the superconducting phase. Contributions at $q_0 \geq q$ will contribute to the neutrino production rate, rather than scattering cross section, when the temperature is near Δ . Analytic results may be obtained for small transfer energies. When q_0 is much smaller than all other energy scales, the vector longitudinal response (see Eq. (A1) of the Appendix) reduces to

$$\begin{aligned} \lim_{q_0 \rightarrow 0} \text{Im} \Pi_L^V(\Delta) &= \frac{2}{1 + e^{\beta\Delta}} \Pi_L^V(\Delta = 0) \\ &= \frac{\mu^2 q_0}{2\pi q} \frac{1}{1 + e^{\beta\Delta}}. \end{aligned} \quad (14)$$

From this the weakening of the low energy, vector-longitudinal response can be calculated for a given gap Δ .

The axial-longitudinal response, which physically corresponds to the excitation of spin waves, is shown in the right panel of Fig. 2. As with the vector channel a threshold of 2Δ is apparent but, unlike the previous case, the response as $q_0 \rightarrow 0$ is *enhanced*. This is manifest in the the limit $q_0 \ll T \sim \Delta$, where one finds [17]

$$\text{Im} \Pi_L^A(\Delta) \simeq \frac{\Delta}{2T} \text{sech}^2 \left(\frac{\Delta}{2T} \right) \ln \left(\frac{\Delta}{q_0} \right) \Pi_L^A(\Delta = 0), \quad (15)$$

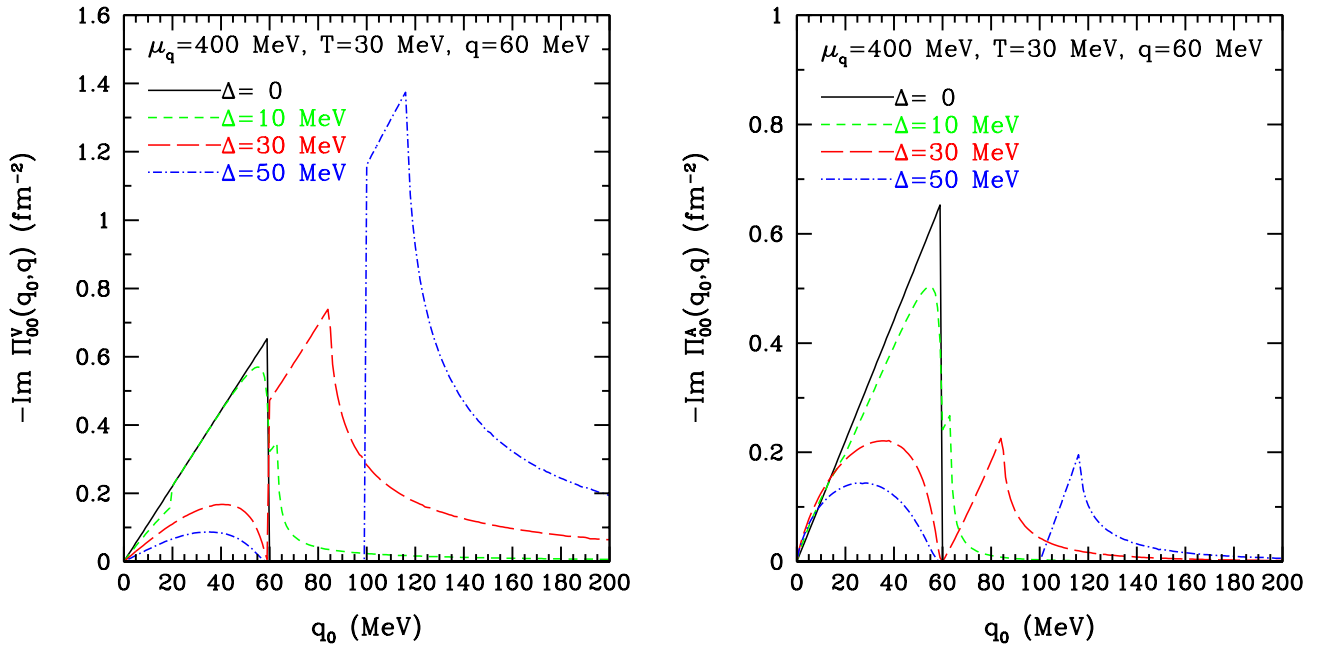


FIG. 2. Vector-longitudinal (left) and axial-longitudinal (right) responses as a function of energy transfer. The momentum transfer is fixed at $q = 50$ MeV.

where in this limit $\Pi_L^A(\Delta = 0) = \mu^2 q_0^2 / 4\pi q$. This logarithmic enhancement will lead to an integrable peak in the differential cross section at $q_0 = 0$, as will be described below.

The transverse response functions, Π_T^V and Π_T^A as defined in Eq. (12), exhibit behavior similar to the longitudinal channels. The primary distinction is that superconductive coherence at low q_0 enhances the vector channel and suppresses the axial. In the former case the interference effects are constructive and in the latter case they are destructive [18], which is a reversal of the longitudinal results. This difference has been theoretically understood and experimentally observed in electric superconductors, where the absorption of acoustic waves (vector-longitudinal) is suppressed while the infra-red absorption (vector-transverse) is enhanced for small energy transfer [19,20]².

In addition to the vector and axial polarizations, the mixed vector-axial polarization (13) also contributes to the cross section. While this contribution is always much smaller – by at least one order of magnitude – we note that it is enhanced in the superconducting phase, leading to an amplified difference between neutrino and anti-neutrino cross sections in PNS matter.

Once the polarization tensors have been computed it is straightforward to obtain the differential cross section, Eq. (2). Results for neutrinos of energy $E_\nu = 50$ MeV, ambient matter conditions of $\mu_q = 400$ MeV and $T = 30$ MeV, and gaps of varied size are plotted as a function of transfer energy in Fig. 3. A striking feature of these results is the singular behavior of the differential cross section near $q_0 = 0$ in superconducting matter. This is the (integrable) logarithmic divergence of Π_L^A and Π_T^V (see (Eq. 15)). The threshold behavior seen in differential cross section, for the case $\Delta = 10$ and 30 MeV, at $q_0 = 2\Delta$ and $q_0 = -2\Delta$ correspond to excitations of the Cooper pairs.

The total cross section (per unit volume) is obtained by integrating over all neutrino energy transfers and angles. From this the mean free path is determined, since

$$\lambda = \left(\frac{\sigma}{V} \right)^{-1}. \quad (16)$$

As suggested by the differential cross section in Fig. 3, the total cross section is reduced in the presence of a gap Δ . The logarithmic peak at $q_0 = 0$ has a minimal effect after integration, when $\Delta \sim T$ and when the neutrino energy $E_\nu \sim \pi T$ since neutrino probe a significant part of the response outside of this $q_0 = 0$ region.

² There is naturally a vast literature concerning coherence effects in superconducting metals, and we find it both gratifying and reassuring to obtain similar results in this less terrestrial context.

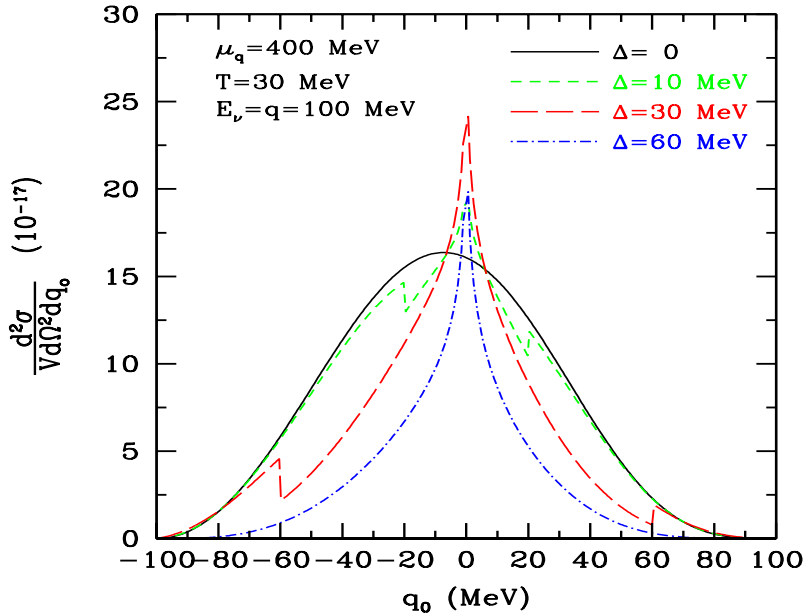


FIG. 3. Differential cross section as a function of energy transfer and for neutrino energy $E_\nu = 50$ MeV.

Results for the neutrino mean free path, λ , are shown in Fig. 4 as a function of incoming neutrino energy E_ν (ambient matter conditions of $\mu_q = 400$ MeV and $T = 30$ MeV have again been used). The same energy dependence has been computed previously in the case of free relativistic and degenerate fermionic matter [13]; it decreases as $1/E_\nu^2$ for $E_\nu \gg T$, and $1/E_\nu$ at $E_\nu \ll T$. The results indicate that this energy dependence is not modified by the presence of a gap when $\Delta \sim T$. Thus the primary effect of the superconducting phase is a much larger mean free path. This is consistent with the suppression found in the vector-longitudinal response function, which dominates the sum polarization sum (10), at $q_0 < q$.

III. THE COOLING OF AN IDEALIZED QUARK STAR

The immediate application of the last section's results is neutrino emission from a proto-neutron star containing quark matter. While we will fall far short of a complete description of the role of color superconductivity in such a complicated environment, in this section we will outline the key ingredients for estimating the possible physical observables. The first subsection describes a simple and general model for the cooling of quark matter through temperatures relevant to proto-neutron stars, and the second addresses the applicability of this scenario to more realistic situations.

A. The Cooling of Superconducting Quark Matter

Having determined the neutrino mean free path in a color superconductor, we now consider the cooling of a macroscopic sphere of quark matter as it becomes superconducting. As stated previously, this toy model is motivated by the possibility that the core of neutron star might contain such matter. Following our preceding calculations, we will consider the relatively simple case of two massless flavors with identical chemical potentials. Furthermore, we will disregard the quarks parallel in color to the condensate; *i.e.* we consider a background comprised exclusively of quasi-quarks.

The cooling of a spherical system of quark matter from $T \sim T_c \sim 50$ MeV is driven by neutrino diffusion, for the neutrino mean free path is much smaller than the dimensions of system of astrophysical size, and yet several orders of magnitude larger than the mean free path of the quarks. The diffusion equation for energy transport by neutrinos in a spherical geometry is

$$C_V \frac{dT}{dt} = -\frac{1}{r^2} \frac{\partial L_\nu}{\partial r}, \quad (17)$$

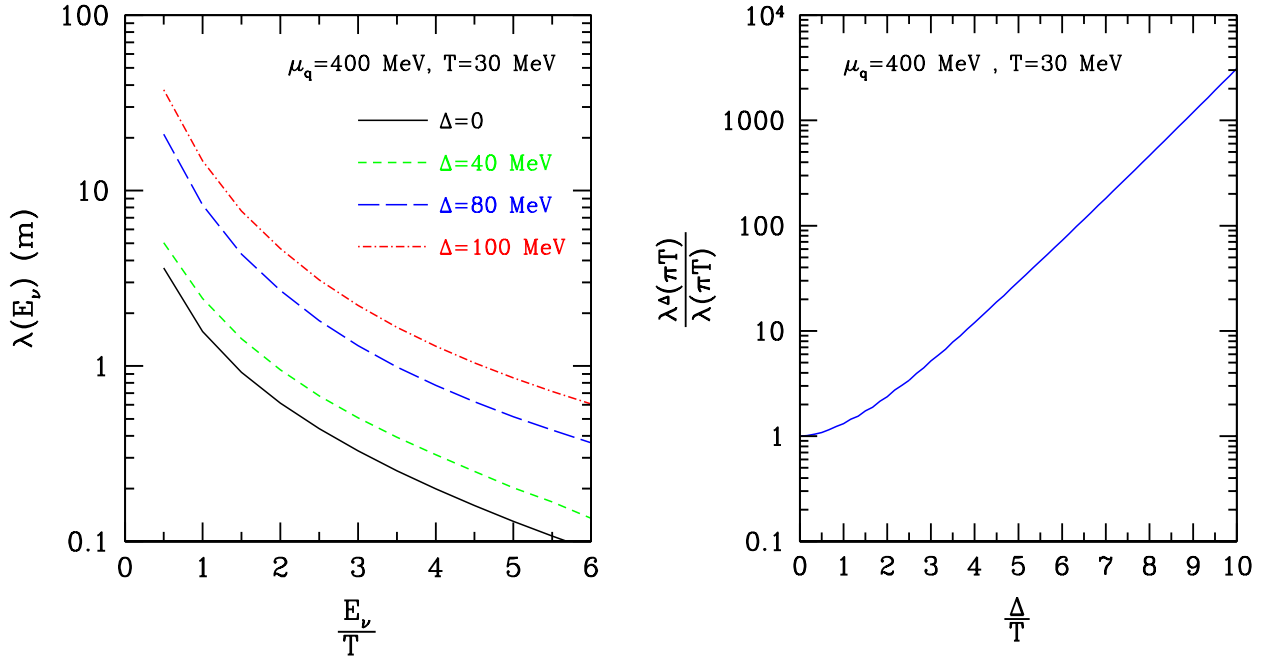


FIG. 4. Left Panel: Neutrino mean free path as a function of neutrino energy. Right Panel: The neutrino mean free path for neutrino energy $E_\nu = \pi T$, plotted as a function of the gap Δ . Results, shown here for $T = 30$ MeV, are virtually independent of temperature for $T \lesssim 50$ MeV.

where C_V is the specific heat per unit volume of quark matter, T is the temperature, and r is the radius. The neutrino energy luminosity for each neutrino type, L_ν , depends on the neutrino mean free path and the spatial gradients in temperature and is approximated by

$$L_\nu \cong -6 \int dE_\nu \frac{c}{6\pi^2} E_\nu^3 r^2 \lambda(E_\nu) \frac{\partial f(E_\nu)}{\partial r}, \quad (18)$$

where c denotes the speed of light in vacuum. In our analysis we assume that neutrino interactions are dominated by the neutral current scattering common to all neutrino types. Consequently, we take the same neutrino and anti-neutrino mean free path for every neutrino flavor, giving rise to the factor of six in Eq. (18). The equilibrium Fermi distribution, $f(E_\nu)$, and the (scattering) mean free path, $\lambda(E_\nu)$, are integrated over all neutrino energies, E_ν .

The solution to the diffusion equation will depend on the size of the system and its initial temperature gradients. However, we are merely interested in a qualitative description of cooling through a second-order phase transition to superconducting matter. The temporal behavior is characterized by a time scale τ_c , which is proportional to the inverse cooling rate and can hence be deduced from Eq. (17). The characteristic time

$$\tau_c(T) = C_V(T) \frac{R^2}{c \langle \lambda(T) \rangle}, \quad (19)$$

is a strong function of the function of the ambient matter temperature since it depends on the matter specific heat and the neutrino mean free path. This applies to a system characterized by the radial length R and the energy-weighted average of the mean free path, $\langle \lambda(T) \rangle$. Following our general treatment of the superconducting gap, we assume that the temperature dependence of the specific heat is described by BCS theory. We will then use the results obtained in the previous section to calculate $\langle \lambda(T) \rangle$. Furthermore, since neutrinos are in thermal equilibrium for the temperatures of interest, we may assume

$$\langle \lambda(T) \rangle \simeq \lambda(E_\nu = \pi T). \quad (20)$$

The quantity on the left is dependent on the gap Δ , a dependence computed in the previous section and plotted in the right panel of Fig. 4. The results indicate that for small Δ/T the neutrino mean free path is not strongly modified, but as Δ/T increases so too does λ , non-linearly at first and then exponentially for $\Delta/T \gtrsim 5$. We note that the diffusion approximation is only valid when $\lambda \ll R$ and will thus fail for very low temperatures, when $\lambda \sim R$.

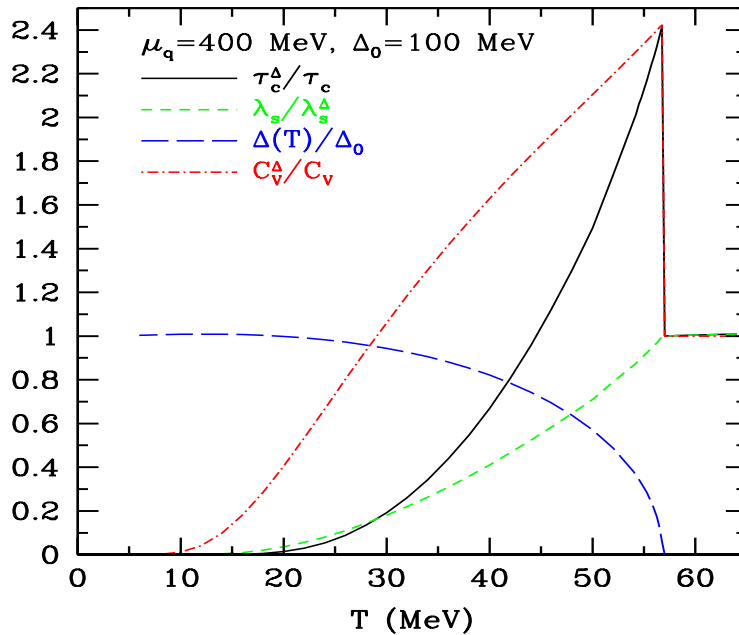


FIG. 5. The figure shows the extent to which different physical quantities are affected due to the superconducting transition. Ratios of the cooling time scale (solid curve), the inverse mean free path (short-dashed curve) and the matter specific heat (dot-dashed curve) in the superconducting phase to that in the normal phase is shown as a function of the matter temperature. The ratio of the gap to its zero temperature value Δ_0 is also shown (long-dashed curve). The quark chemical potential is $\mu_q = 400$ MeV and $\Delta_0 = 100$ MeV.

The ratio $\tau_c^\Delta(T)/\tau_c(T)$, a measure of the extent to which the cooling rate is changed by a gap, is shown by the solid line in Fig. 5. The ratio λ/λ^Δ , plotted with the short-dashed curve, measures the decrease in neutrino interaction rates in the superconducting background. The temperature dependences we have taken from BCS theory, that of the specific heat (dashed curve) and the magnitude of the gap itself (dot-dashed curve), are shown for reference in Fig. 5. The results shown in Fig. 5 are readily interpreted. The cooling rate around T_c is influenced mainly by the peak in the specific heat associated with the second order phase transition, since the neutrino mean free path is not strongly affected when $\Delta \ll T$. Subsequently, as the matter cools, both C_V and λ^{-1} decrease in a non-linear fashion for $\Delta \sim T$. Upon further cooling, when $\Delta \gg T$, both C_V and λ^{-1} decrease exponentially. Both of these effects accelerate the cooling process.

We conclude that if it were possible to measure the neutrino luminosity from the hypothetical object described here, a unique temporal profile would be observed. This suggests that if a second order, superconducting transition were to occur inside a proto-neutron star it could be identified by the temporal characteristics of the late time supernova neutrino signal. Specifically, there would be a brief interval during which the cooling would slow around $T \sim T_c$, signified by a period of reduced neutrino detection.

B. Relation to Proto-Neutron Stars

The temporal pattern of neutrino emission deduced here would be observable evidence of the onset of color superconductivity in dense matter. However, ours is a simple model, and we must temper our speculations with considerations of more realistic systems.

Neutrinos emitted from the core of a proto-neutron star, be it hadronic or quark matter in any phase, must pass through a large amount of matter in the outer shell. The neutron-rich material is characterized in the outer shell is opaque to neutrinos and will thus even out any sharp temporal features associated with the interior emission. This is the first and foremost of caveats since this will directly impact the possibility of observing a characteristic in the neutrino signal associated with the phase transition.

As discussed in Section II, the scalar diquark condensate in a two-flavor color superconductor is necessarily colored. Therefore quarks of one color, taken conventionally as color 3, will be color-orthogonal to the scalar condensate and can remain ungapped. We have not included these color-3 quarks in our analysis of neutrino scattering since their

fate is uncertain [21]; they could form color-symmetric Cooper pairs, or perhaps a chiral condensate. If we take the simplest scenario and assume that they remain free, their presence in the medium will further dilute any direct effects of the gapped quasi-quarks. Specifically, the physical quantities in plotted in Fig. 5 will not vanish when $T \rightarrow 0$, instead being reduced to one third of their $\Delta = 0$ values. Likewise, the maxima at T_c will be reduced relative to a color-neutral background.

The second-order phase transition is taken directly from BCS theory, which we assume rather than derive. While this is the mean-field result for two massless flavors with equivalent chemical potentials, neutron star matter is constrained in two ways. First of all, weak-interaction equilibrium requires $\mu_d - \mu_u = \mu_e$, where the subscripts refer to down quarks, up quarks, and electrons. But since a finite electron number is required to achieve electric charge neutrality in the star, μ_e cannot vanish and we necessarily have $\mu_d \neq \mu_u$. This difference in chemical potentials is likely to drive a first order rather than a BCS-second order transition [22].

The other notable omission in our study is the strange quark. As before, weak interaction equilibrium requires that $\mu_s = \mu_d$, and thus for $\mu_d \gtrsim m_s$ strange quarks will be present. Furthermore, the finite strange quark mass implies a mismatch in the Fermi momenta which would also drive a first order transition [4]. A generic consequence of a first order transition is a mixed phase containing both normal and superconducting quark matter, and transport in the heterogeneous mixed phase is qualitatively different from that considered here, for neutrino scattering will depend on the size and nature of the structures (droplets) present. In previous work it was shown that neutrino mean free path in the heterogeneous phase can be greatly reduced due to coherent scattering of droplets in the mixed phase [23]. Combining the results of Section II with neutrino transport in a mixed phase of superconducting and normal quark matter is beyond the scope of this work.

Therefore, while our calculation of the neutrino mean free path will be an essential ingredient in a more realistic and hence more complicated model of neutron star evolution, our toy model only applies to a highly idealized quark core of a neutron star where $\Delta \gg |\mu_d - \mu_u|$.

IV. CONCLUSIONS

Motivated by the physical relevance of neutrino diffusion in the cooling of strongly-interacting matter, we have analyzed the effects on neutrino-quark scattering arising from a second-order phase transition from normal to color superconducting quark matter. The principal microscopic ingredient is the neutrino mean free path, and this was calculated in linear-response theory with a BCS-type superconducting background. We then applied this result to a schematic model of quark matter at temperatures and densities relevant to the evolution of proto-neutron stars. The modified mean free path for neutrinos in a superconducting background was computed in the simplified approximation of iso-symmetric, two-flavor quark matter. We have enumerated the main shortcomings of these simplifications and realize that a more realistic treatment of PNS evolution would include many other effects of similar importance.

Despite these caveats, our toy model calculation indicates that a superconducting transition in the quark core of a PNS can impact its early cooling and thereby potentially alter the temporal characteristics of the neutrino emission. We view this work as a first step towards an understanding of how the presence of color superconducting matter in the core of a neutron star may affect the early – and observable – neutrino signal. Quark pairing invariably occurs in theoretical treatments of finite-density QCD, and thus our microscopic calculations of the neutrino cross sections are pertinent to transport processes in dense quark matter. Given the real prospect of detecting neutrinos emitted from a future supernova event, such transport processes might someday serve as an probe of the properties of extremely dense matter.

V. ACKNOWLEDGMENTS

We thank the organizers of the INT Program on QCD at Finite Baryon Density, during which this work was begun, and G.W.C. thanks the Institute for Nuclear Theory for their hospitality. We also thank David Kaplan, M. Prakash, Krishna Rajagopal, and Martin Savage for critical readings of the manuscript and for useful comments. This work was supported by the US Department of Energy grants DE-FG02-88ER40388 (G.W.C.) and DE-FG03-00-ER41132 (S.R.).

APPENDIX: QUARK POLARIZATION TENSORS

At densities relevant to this work, only the quark particle-hole excitations are accessible. Thus we discard all anti-particle and anti-hole contributions from the propagators in Eqs. (6) and (8).

The imaginary part of the vector longitudinal polarization is, for each flavor,

$$\begin{aligned}
\text{Im } \Pi_{00}^V(q_0, q) &= -2\pi \int \frac{d^3p}{(2\pi)^3} \frac{d^3k}{(2\pi)^3} \delta^3(p - k - q)(1 + \hat{p} \cdot \hat{k}) \\
&\times \left\{ [n(\xi_p) - n(\xi_k)] \left[\delta(q_0 + \xi_p - \xi_k) \frac{(\xi_p + E_p)(\xi_k + E_k) - \Delta^2}{4\xi_p\xi_k} \right. \right. \\
&\quad \left. \left. - \delta(q_0 - \xi_p + \xi_k) \frac{(\xi_p - E_p)(\xi_k - E_k) - \Delta^2}{4\xi_p\xi_k} \right] \right. \\
&\quad \left. + [1 - n(\xi_p) - n(\xi_k)] \left[\delta(q_0 - \xi_p - \xi_k) \frac{(\xi_p - E_p)(\xi_k + E_k) + \Delta^2}{4\xi_p\xi_k} \right. \right. \\
&\quad \left. \left. - \delta(q_0 + \xi_p + \xi_k) \frac{(\xi_p + E_p)(\xi_k - E_k) + \Delta^2}{4\xi_p\xi_k} \right] \right\}. \tag{A1}
\end{aligned}$$

The axial longitudinal differs only in the sign of the anomalous Δ^2 term, a consequence of coherence effects being different in different channels, and is given by

$$\begin{aligned}
\text{Im } \Pi_{00}^A(q_0, q) &= -2\pi \int \frac{d^3p}{(2\pi)^3} \frac{d^3k}{(2\pi)^3} \delta^3(p - k - q)(1 + \hat{p} \cdot \hat{k}) \\
&\times \left\{ [n(\xi_p) - n(\xi_k)] \left[\delta(q_0 + \xi_p - \xi_k) \frac{(\xi_p + E_p)(\xi_k + E_k) + \Delta^2}{4\xi_p\xi_k} \right. \right. \\
&\quad \left. \left. - \delta(q_0 - \xi_p + \xi_k) \frac{(\xi_p - E_p)(\xi_k - E_k) + \Delta^2}{4\xi_p\xi_k} \right] \right. \\
&\quad \left. + [1 - n(\xi_p) - n(\xi_k)] \left[\delta(q_0 - \xi_p - \xi_k) \frac{(\xi_p - E_p)(\xi_k + E_k) - \Delta^2}{4\xi_p\xi_k} \right. \right. \\
&\quad \left. \left. - \delta(q_0 + \xi_p + \xi_k) \frac{(\xi_p + E_p)(\xi_k - E_k) - \Delta^2}{4\xi_p\xi_k} \right] \right\}. \tag{A2}
\end{aligned}$$

From these expressions, one may obtain $\Pi_{11}^{V,A}$, $\Pi_{10}^{V,A}$, and $\Pi_{01}^{V,A}$ as specified in Eq. (11).

The transverse response functions have similar forms. The vector is

$$\begin{aligned}
\text{Im } \Pi_{22}^V(q_0, q) &= -2\pi \int \frac{d^3p}{(2\pi)^3} \frac{d^3k}{(2\pi)^3} \delta^3(p - k - q)(1 + \hat{p} \cdot \hat{k} - 2\hat{p}_2\hat{k}_2) \\
&\times \left\{ [n(\xi_p) - n(\xi_k)] \left[\delta(q_0 + \xi_p - \xi_k) \frac{(\xi_p + E_p)(\xi_k + E_k) + \Delta^2}{4\xi_p\xi_k} \right. \right. \\
&\quad \left. \left. - \delta(q_0 - \xi_p + \xi_k) \frac{(\xi_p - E_p)(\xi_k - E_k) + \Delta^2}{4\xi_p\xi_k} \right] \right. \\
&\quad \left. + [1 - n(\xi_p) - n(\xi_k)] \left[\delta(q_0 - \xi_p - \xi_k) \frac{(\xi_p - E_p)(\xi_k + E_k) - \Delta^2}{4\xi_p\xi_k} \right. \right. \\
&\quad \left. \left. - \delta(q_0 + \xi_p + \xi_k) \frac{(\xi_p + E_p)(\xi_k - E_k) - \Delta^2}{4\xi_p\xi_k} \right] \right\}, \tag{A3}
\end{aligned}$$

and the axial,

$$\begin{aligned}
\text{Im } \Pi_{22}^A(q_0, q) &= -2\pi \int \frac{d^3p}{(2\pi)^3} \frac{d^3k}{(2\pi)^3} \delta^3(p - k - q) (1 + \hat{p} \cdot \hat{k} - 2\hat{p}_2 \hat{k}_2) \\
&\times \left\{ [n(\xi_p) - n(\xi_k)] \left[\delta(q_0 + \xi_p - \xi_k) \frac{(\xi_p + E_p)(\xi_k + E_k) + \Delta^2}{4\xi_p \xi_k} \right. \right. \\
&\quad \left. \left. - \delta(q_0 - \xi_p + \xi_k) \frac{(\xi_p - E_p)(\xi_k - E_k) + \Delta^2}{4\xi_p \xi_k} \right] \right. \\
&\quad \left. + [1 - n(\xi_p) - n(\xi_k)] \left[\delta(q_0 - \xi_p - \xi_k) \frac{(\xi_p - E_p)(\xi_k + E_k) - \Delta^2}{4\xi_p \xi_k} \right. \right. \\
&\quad \left. \left. - \delta(q_0 + \xi_p + \xi_k) \frac{(\xi_p + E_p)(\xi_k - E_k) - \Delta^2}{4\xi_p \xi_k} \right] \right\}. \tag{A4}
\end{aligned}$$

Finally, there is a small but finite response in the mixed vector-axial channel. Since the neutrino tensor element L^{23} is imaginary, we take the real part of the polarization. Antisymmetric in spin, it is

$$\begin{aligned}
\text{Re } \Pi_{23}^{VA}(q_0, q) &= -2\pi \int \frac{d^3p}{(2\pi)^3} \frac{d^3k}{(2\pi)^3} \delta^3(p - k - q) (\hat{p}_1 - \hat{k}_1) \\
&\times \left\{ [n(\xi_p) - n(\xi_k)] \left[\delta(q_0 + \xi_p - \xi_k) \frac{(\xi_p + E_p)(\xi_k + E_k) + \Delta^2}{4\xi_p \xi_k} \right. \right. \\
&\quad \left. \left. - \delta(q_0 - \xi_p + \xi_k) \frac{(\xi_p - E_p)(\xi_k - E_k) + \Delta^2}{4\xi_p \xi_k} \right] \right. \\
&\quad \left. + [1 - n(\xi_p) - n(\xi_k)] \left[\delta(q_0 - \xi_p - \xi_k) \frac{(\xi_p - E_p)(\xi_k + E_k) - \Delta^2}{4\xi_p \xi_k} \right. \right. \\
&\quad \left. \left. - \delta(q_0 + \xi_p + \xi_k) \frac{(\xi_p + E_p)(\xi_k - E_k) - \Delta^2}{4\xi_p \xi_k} \right] \right\}. \tag{A5}
\end{aligned}$$

- [1] B. C. Barrois, Nucl. Phys. **B129**, 390 (1977).
S. C. Frautschi, in *Workshop on Hadronic Matter at Extreme Energy Density*, Erice, Italy, Oct 13-21, 1978.
D. Bailin and A. Love, Phys. Rept. **107**, 325 (1984).
- [2] M. Alford, K. Rajagopal, and F. Wilczek, Phys. Lett. **B422**, 247 (1998).
R. Rapp, T. Schäfer, E. V. Shuryak, and M. Velkovsky, Phys. Rev. Lett. **81**, 53 (1998).
- [3] J. Berges and K. Rajagopal, Nucl. Phys. **B538**, 215 (1999).
G. W. Carter and D. Diakonov, Phys. Rev. **D60**, 016004 (1999).
- [4] M. Alford, K. Rajagopal, and F. Wilczek, Nucl. Phys. **B537**, 443 (1999).
M. Alford, J. Berges, and K. Rajagopal, Nucl. Phys. **B558**, 219 (1999).
T. Schäfer and F. Wilczek, Phys. Rev. **D60**, 074014 (1999).
- [5] R. D. Pisarski and D. H. Rischke, Phys. Rev. **D60**, 094013 (1999).
R. D. Pisarski and D. H. Rischke, Phys. Rev. **D61**, 074017 (2000).
D. H. Rischke, nucl-th/0001040.
M. Rho, A. Wirzba, and I. Zahed, Phys. Lett. **B473**, 126 (2000).
M. Rho, E. Shuryak, A. Wirzba, and I. Zahed, hep-ph/0001104.
- [6] D. T. Son, Phys. Rev. **D59**, 094019 (1999).
- [7] S. R. Beane, P. F. Bedaque, and M. J. Savage, nucl-th/0004013.
- [8] S. A. Colgate and R. H. White, Astrophys. J., **143**, 626 (1966).
V. S. Imshennik and D. K. Nadyozhin, Soviet Physics JETP **36**, 821 (1973).
A. Burrows and J. M. Lattimer, Astrophys. J., **307**, 178 (1986).
W. Keil and H. T. Janka, Astronomy and Astrophysics, **296**, 145 (1995),

- J. Pons et al., *Astrophys. J.*, **513**, 513 (1999).
- [9] M. Prakash, I. Bombaci, M. Prakash, P. J. Ellis, J. M. Lattimer, and R. Knorren, *Phys. Rep.* **280**, 1 (1997).
 - [10] M. Alford, J. Berges, and K. Rajagopal, *Nucl. Phys.* **B571**, 269 (2000).
 - [11] D. Page, M. Prakash, J. M. Lattimer, and A. Steiner, hep-ph/0005094.
D. Blaschke, T. Klähn, and D. N. Voskresensky, astro-ph/9908334.
 - [12] C. J. Horowitz and K. Wehrberger, *Nucl. Phys.* **A531**, 665 (1991); *Phys. Lett.* **B226**, 236 (1992).
 - [13] S. Reddy, M. Prakash, and J. M. Lattimer, *Phys. Rev.* **D58**, 013009 (1998).
 - [14] J. Bardeen, L. N. Cooper, and J. R. Schrieffer, *Phys. Rev.* **108**, 1175 (1957).
 - [15] R. D. Pisarski and D. H. Rischke, *Phys. Rev.* **D61**, 051501 (2000).
 - [16] J. Fetter and J. D. Walecka, *Quantum Theory of Many Particle Systems*, (McGraw-Hill, New York, 1979).
 - [17] E. M. Lifshitz and L. P. Pitaevskii, *Physical Kinetics*, (Pergamon Press, Oxford, 1981).
 - [18] J. Bardeen and J. R. Schrieffer, in *Progress in Low Temperature Physics*, (North-Holland, Amsterdam, 1961), Vol III.
 - [19] D. C. Mattis and J. Bardeen, *Phys. Rev.* **111**, 412 (1958).
 - [20] L. H. Palmer and M. Tinkham, *Phys. Rev.* **165**, 588 (1968).
 - [21] F. Sannino, hep-ph/0002277.
 - [22] P. Bedaque, hep-ph/9910247.
 - [23] S. Reddy, G. F. Bertsch, and M. Prakash, *Phys. Lett.* **B475**, 1 (2000).